

# Dynamic characterization of intensity fluctuations in semiconductor lasers under digital modulation

メタデータ	言語: eng 出版者: 公開日: 2017-10-03 キーワード (Ja): キーワード (En): 作成者: メールアドレス: 所属:
URL	<a href="http://hdl.handle.net/2297/3728">http://hdl.handle.net/2297/3728</a>

## Dynamic Characterization of Intensity Fluctuations in Semiconductor Lasers under Digital Modulation

Moustafa Ahmed<sup>1</sup>, Minoru Yamada<sup>2</sup>

<sup>1</sup>Minia University, Egypt; <sup>2</sup>Kanazawa University, Japan  
[m.farghal@link.net](mailto:m.farghal@link.net)

### Abstract

We report on modeling of intensity fluctuations in semiconductor lasers subject to low and high speed digital modulation. We examine influence of deciding both decision and sampling times on bit-error-rate (BER). Correlation between BER and relative intensity noise (RIN) is presented.

**Keywords:** Bit error rate, digital modulation, fluctuation, noise, semiconductor lasers.

### 1. Introduction

Intensity fluctuations represent an important parameter to criticize performance of semiconductor laser applications. It is common to characterize the noise content of fluctuations in terms of RIN. However, when the laser is utilized as a radiation source in digital systems, intensity fluctuations should be determined in terms of BER. Determination of operating conditions that correspond to minimum levels of fluctuations and BER is very important for both cases of free- and above-threshold biasing [1]. The former is desired to reduce consumption power, while the latter is commonly used for high speed modulation in order to avoid BER degradation due to enhanced intensity fluctuations. Dynamic response of laser in digital systems is qualitatively examined by the visual eye diagram. The BER is examined by sampling intensity fluctuations in both “on” and “off” states over an optional period, and then determining the probabilities  $P(\text{on/off})$  and  $P(\text{off/on})$  of incorrect counting of “on” and “off” states, respectively. By scanning this sampling time along the bit slot at definite times, called “decision times”, the BER is decided as the minimum average value of  $P(\text{on/off})$  and  $P(\text{off/on})$ . Although optimum choices of the sampling and decision times are critical in determining BER, their modeling has received inadequate theoretical consideration. Moreover, it often happens that intensity fluctuations are measured in terms of RIN in digital systems, which perhaps due to rather cheap measuring setups. Therefore correlation between RIN and BER is necessary.

In this paper, we characterize intensity fluctuations of both low and high speed

modulated lasers in terms of the eye diagram and BER. We criticize the optimum sampling and decision times. Both cases of biasing-free and above-threshold biasing are considered. We also study influence of nonlinear gain, as an important modulation parameter on BER.

### 2. Theoretical Model

Laser dynamics are described by the rate equations of the photon number  $S(t)$  and injected electron number  $N(t)$ : [2]

$$\frac{dS}{dt} = [A - BS - G_{th}]S + \frac{a\xi}{V}N + F_S(t) \quad (1)$$

$$\frac{dN}{dt} = \frac{I}{e} - AS - \frac{N}{\tau_s} + F_N(t) \quad (2)$$

$G_{th}$  is the threshold gain,  $A$  and  $B$  are coefficients for linear and nonlinear gain,  $a$  and  $\xi$  are parameters of linear gain,  $V$  is volume of active region,  $\tau_s$  is spontaneous emission lifetime. The injected current  $I$  is composed of dc-biasing current  $I_b$  and modulation current  $I_m$ :

$$I = I_b + I_m * (\text{NRZ - pulse code}) \quad (3)$$

The pulse train is generated by a  $2^7-1$  virtual random bit-code generator. The terms  $F_S(t)$  and  $F_N(t)$  are Langevin noise sources that account for intrinsic fluctuations of  $S(t)$  and  $N(t)$ .

Equations (1) and (2) are numerically solved by the fourth-order Runge-Kutta method with a time step of 2ps. Two bit-slots are used with periods  $T_b=0.5\text{ns}$  (low speed modulation) and 0.1ns (high speed) that correspond to bit frequencies lower and higher than the relaxation frequency, respectively. The noise sources are generated following our model in [2]. The eye diagram is constructed by dividing the stream of  $S(t)$  into segments of length  $3T_b$  and superposing them. BER is calculated as follows. The photon numbers  $S_{on}(t)$  and  $S_{off}(t)$  are sampled over different periods  $0 \leq T_s \leq T_b$  and at possible decision times  $0 \leq T_d \leq T_b$  as shown in Fig. 1(a). For each pair of  $T_s$  and  $T_d$ , the variances of fluctuations of  $S_{on}(t)$  and  $S_{off}(t)$  are examined. These variances are then used to calculate the error probabilities  $P(\text{on/off})$  and  $P(\text{off/on})$  taking into account shot and circuit noises in the detector end and assuming Gaussian statistics of

the received signal [1]. BER is then calculated as the minimum average of  $[P(\text{on/off}) + P(\text{off/on})]/2$ . RIN is calculated from fluctuations of  $S_{\text{on}}(t)$  and  $S_{\text{off}}(t)$  during the optimum times  $T_s$  and  $T_d$ , as illustrated in [2]. In calculations, we considered AlGaAs lasers with threshold current  $I_{th}=11.3\text{mA}$ ,  $V=48\mu\text{m}^3$ ,  $a=2.75\times 10^{-12}\text{s}^{-1}$ ,  $\zeta=0.15$  and  $\tau_s=2\text{ns}$ .

### 3. Results and Discussion

Figs. 1(a) and (b) plot the eye diagrams simulated for bit slots  $T_b=0.1$  and  $0.5\text{ns}$ , respectively, when  $I_b=I_m=2.0I_{th}$ . The figures indicate that timing jitters are displayed on the eye diagram of the shorter slot case, and the eye is less opened. Fig. 2 plots the BER values associated with the case of  $T_b=0.1$  as functions of  $T_d$  and  $T_s$ . The figure indicates that minimum values of BER are obtained for longer  $T_s$  and intermediate  $T_d$ . In the case of  $T_b=0.5\text{ns}$ , these optimum values change to larger values of both  $T_s$  and  $T_d$ .

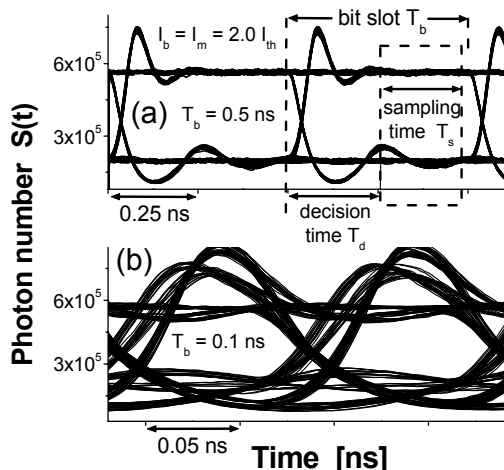


Fig. 1. Eye diagrams simulated for bit slots: (a)  $T_b=0.1$  ns and (b)  $T_b=0.5$  ns, when  $I_b=I_m=2.0I_{th}$ .

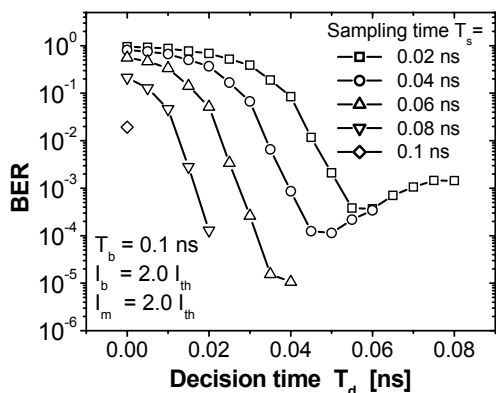


Fig. 2. Influence of deciding  $T_b$  and  $T_s$  on BER.

Influence of biasing current  $I_b$  on BER is illustrated in Fig. 3. The corresponding variation

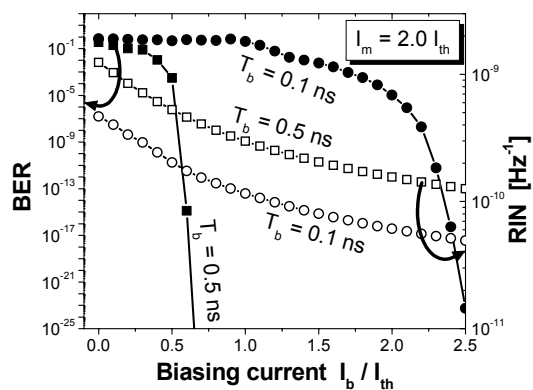


Fig. 3. Influence of  $I_b$  on both BER and RIN.

of low-frequency RIN is plotted on the right-hand axis. BER is high for low current  $I_b$  and then decreases rapidly when  $I_b > 0.5I_{th}$  for  $T_b=0.5\text{ns}$  and when  $I_b > 2.0I_{th}$  for  $T_b=0.1\text{ns}$ . RIN, however, decreases smoothly with increase of  $I_b$ , and the longer slot case attains higher RIN. Influence of nonlinear gain on BER is illustrated in Fig. 4 as a function of  $I_d$ . As shown, nonlinear gain has a little effect on BER when  $T_b=0.5\text{ns}$ , whereas it enhances BER for current  $I_b > I_{th}$  when  $T_b=0.1\text{ns}$ . This is because nonlinear gain works to suppress the relaxation oscillations that dominate the eye diagram of slot  $T_b=0.1\text{ns}$ , as shown in Fig. 1.

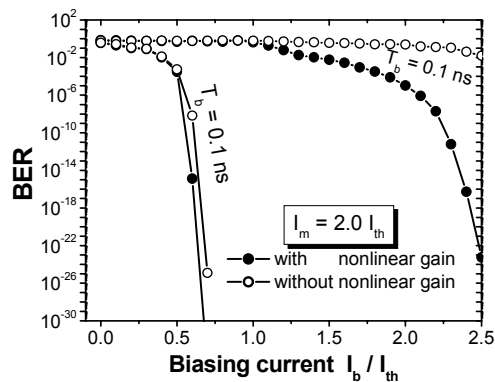


Fig. 4. Influence on nonlinear gain on BER.

### Acknowledgement

The authors wish to thank Dr. Richard Schatz at KTH, Sweden, Dr. Johan Gustavsson at Chalmers University of Technology, Sweden, and Dr. Rainer Michalizk at Ulm University, Germany for valuable discussions.

### References

- 1) G. P. Agrawal, Fiber-optic communication systems, Van Nostrand Reinhold, New York, 2003.
- 2) M. Ahmed, M. Yamada and M. Saito, IEEE J. Quantum Electron. 37, 1600-1610, 2001.